Density-density response of dilute ^{3}He-^{4}He mixtures at low temperatures

M. Weyrauch
Physikalisch-Technische Bundesanstalt, 38116 Braunschweig, Federal Republic of Germany

A. Szprynger
Institute of Low Temperature and Structure Research, Polish Academy of Science, 50-950 Wrocław, Poland
(Received 15 August 1994)

An attempt is made to describe the dynamical structure factors of ^{3}He-^{4}He mixtures recently measured by Fåk *et al.* [Phys. Rev. B **41**, 8732 (1990)] in the polarization potential approach, which is formulated to include the structure factor S_{34}. Good qualitative agreement of calculation and data is achieved. It turns out that virtual phonon-roton excitations provide significant strength to the particle-hole peak of the structure function and that virtual quasiparticle-quasihole excitations contribute significantly to the phonon-roton peak.

I. INTRODUCTION

Dilute solutions of ^{3}He in ^{4}He are interesting Fermi liquids whose Fermi momentum can be varied by changing the ^{3}He concentration. They provide us with a means to study Fermi liquids at densities not attainable by the pure system. The properties of this unique type of Fermi liquid have been investigated since the early 1960s mostly by thermodynamic measurements. From those data Bardeen, Baym, and Pines, in a pioneering work,[1] determined the effective interaction between the ^{3}He quasiparticles in dilute solutions. The interaction turns out to be weak and attractive at low wavelength, and it is obtained as the sum of the strongly repulsive "direct" interaction between the ^{3}He quasiparticles and the equally strong attractive "indirect" phonon exchange interaction.

Neutron-scattering experiments are able to map out the structure factor $S(\mathbf{q},\omega)$ in a wide range of momentum transfer $\mathbf{q}$ and energy transfer ω. Focus of the first neutron-scattering experiments on ^{3}He-^{4}He mixtures was the phonon-roton peak of the structure factor and its shift relative to the position of this peak in pure ^{4}He.[2,3] Theoretical investigations of the structure factor also concentrated on this shift.[4–6] Recently high-quality data became available in a wide range of momentum and energy transfers.[7] A typical data set is reproduced in Fig. 1. It clearly shows two distinct peaks: the lower energy peak is usually called particle-hole peak, since it is assumed that it essentially stems from ^{3}He quasiparticle-quasihole excitations. The higher energy peak is generally attributed to collective phonon-roton excitations. In this work we will show that virtual phonon-roton excitations contribute significantly to the lower energy peak, and that, conversely, virtual quasiparticle-quasihole excitations provide significant strength to the higher energy peak of the structure function. This is the consequence of a strong ^{3}He-^{4}He interaction.

The calculation is performed within the polarization potential approach proposed by Pines and co-workers. The polarization potentials determined for pure ^{3}He (Ref. 8) and ^{4}He (Ref. 9) are suitably extrapolated for the calculation of ^{3}He-^{4}He mixtures. Our approach describes qualitatively well the data of Fåk *et al.*[7] in a wide range of momentum and energy transfers. Most striking is the very significant contribution of the interference term S_{34} to both peaks of the structure function. Moreover, the decrease of strength in the lower energy peak with increasing momentum transfer observed in the data is reproduced by this calculation.

Previous work within a similar approach has been done by Pedersen and Cowley[5] and Hsu, Pines, and Aldrich.[6] However, there are many differences to the present work which will be outlined in the following. Lücke and Szprynger[4] calculated structure factors for the kinematic region around of the roton minimum using a very different approach. A qualitative discussion of the role S_{34} guided by sum-rule calculations has been recently published by Boronat *et al.*[10]

II. STRUCTURE FACTOR, SUSCEPTIBILITY, AND CROSS SECTION

The inelastic neutron-scattering cross section for unpolarized neutrons is related to the structure factor $S(\mathbf{q},\omega)$ by

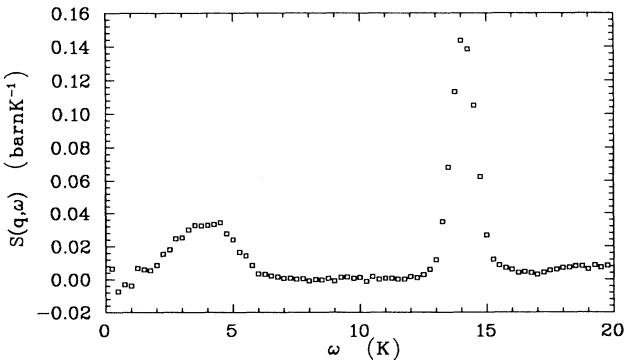

FIG. 1. Measured spectrum at $q=11$ nm^{-1} for a 5% mixture at temperature $T=0.07$ K and density $n=21.97$ nm^{-3} (Ref. 7).

$$\frac{d\sigma}{d\Omega' dE'} = \frac{N}{4\pi}\frac{k'}{k} S(\mathbf{q},\omega) \ . \tag{2.1}$$

Here, $\mathbf{k}$, E and $\mathbf{k}'$, E' are the momentum and energy of the incoming and scattered neutrons, respectively; $\mathbf{q}=\mathbf{k}'-\mathbf{k}$ is the momentum transfer and $\omega=E'-E$ is the energy transfer to the sample. The total number of helium atoms contained in the sample with volume V is denoted by $N=N_3+N_4$; the corresponding particle density is $N/V=n=n_3+n_4$. We furthermore introduce the concentration x_3 of the ^{3}He atoms in the mixture so that $n_3=x_3 n$ and $n_4=(1-x_3)n$. Units are chosen such that Boltzmann's constant $k_B=1$ and Planck's constant $\hbar=1$.

For a ^{3}He-^{4}He mixture the structure factor can be separated into four terms,[11]

$$S(\mathbf{q},\omega)=\sigma_4^c S_{44}^c(\mathbf{q},\omega)+2\sigma_{34}^c S_{34}^c(\mathbf{q},\omega) + \sigma_3^c S_{33}^c(\mathbf{q},\omega)+\sigma_3^i S_{33}^i(\mathbf{q},\omega) \ , \tag{2.2}$$

with σ^c the coherent and σ^i the incoherent nuclear scattering cross section. These cross sections and the interference term σ_{34}^c can be expressed in terms of the scattering lengths b^c and b^i by $\sigma^{c/i}=4\pi|b^{c/i}|^2$ and $\sigma_{34}^c=4\pi\,\mathrm{Re}(b_3^c b_4^c)$. Measured values for the scattering lengths[12] used in this paper are $b_3^c=5.74(7)-1.483(2)i$ fm, $b_3^i=1.7(2)+2.568(3)i$ fm; $b_4^c=3.26(3)$ fm and $b_4^i=0$, since ^{4}He has spin zero. The values in parentheses are the uncertainties in the last digit. As is obvious the real part of b_3^i is rather uncertain; a new measurement is presently under way.[13]

The separation of $S(\mathbf{q},\omega)$ into S_{44}^c, S_{34}^c, S_{33}^c, and S_{33}^i is theoretical, and only $S(\mathbf{q},\omega)$ can be determined experimentally. The structure factor is related to the imaginary part of the (retarded) dynamic susceptibility $\chi(\mathbf{q},\omega)=\chi'(\mathbf{q},\omega)+i\chi''(\mathbf{q},\omega)$ via the fluctuation dissipation theorem ($i,j\in\{3,4\}$)

$$S_{ij}(\mathbf{q},\omega)=-\frac{\chi_{ij}''(\mathbf{q},\omega)}{n\pi(1-e^{-\omega/T})} \tag{2.3}$$

with T denoting the temperature. The susceptibilities are written in terms of the density operator $\rho_i(\mathbf{q},t)=\sum_k \exp[i\mathbf{q}\mathbf{r}_k(t)]$, where the sum extends over all particles at positions $\mathbf{r}_k$ of species i:

$$\chi_{ij}^c(\mathbf{q},\omega)=-\frac{i}{V}\int_0^\infty dt e^{i\omega t}\langle 0|[\rho_i(\mathbf{q},t),\rho_j(-\mathbf{q},0)]|0\rangle \ , \tag{2.4}$$

$|0\rangle$ denotes the ground state of the mixture.

Analogously, for $\chi_{33}^i(\mathbf{q},\omega)$ the density operator in Eq. (2.4) is replaced by the spin-density operator $\vec{I}_3(\mathbf{q},t)=\frac{1}{2}\sum_k \vec{\sigma}_k \exp[i\mathbf{q}\mathbf{r}_k(t)]$:

$$\chi_{33}^i(\mathbf{q},\omega)=-\frac{4i}{3V}\int_0^\infty dt e^{i\omega t}\langle 0|[\vec{I}_3(\mathbf{q},t);\vec{I}_3(-\mathbf{q},0)]|0\rangle \ . \tag{2.5}$$

The Pauli matrices are denoted by $\vec{\sigma}$. In the following we shall assume that the sample is isotropic, so that all susceptibilities and structure functions depend on $q=|\mathbf{q}|$ only, and that $\vec{I}_3\vec{I}_3$ in Eq. (2.5) can be replaced by $3I_3^z I_3^z$ with z indicating the third component in spin space.

III. POLARIZATION POTENTIAL APPROACH

Ab initio calculations of Eqs. (2.4) and (2.5) for ^{3}He-^{4}He mixtures are extremely difficult. Therefore, Pines and coworkers[6,8,9] have advocated the polarization potential approach to determine the susceptibilities. The polarization potential approach utilizes semiphenomenologically determined parameters to describe experimental data within a simple intuitive framework. This procedure has been successful for pure ^{3}He (Ref. 8) and ^{4}He;[9] it is formally equivalent to standard random-phase approximation. We will use this approach to calculate the susceptibilities of ^{3}He-^{4}He mixtures. Related work has been done previously by Pedersen and Cowley[5] and by Hsu, Pines, and Aldrich.[6]

In the polarization potential approach the susceptibility $\bar{\chi}_{44}^c$ of pure ^{4}He is obtained from

$$\bar{\chi}_{44}^c(q,\omega)=\frac{\chi_{44}^{0,c}(q,\omega)}{1-V_{44}(q,\omega)\chi_{44}^{0,c}(q,\omega)+i\epsilon} \ . \tag{3.1}$$

Here $V_{44}(q,\omega)$ is the polarization potential to be discussed in more detail in the following section. The "screened" susceptibility $\chi_{44}^{0,c}(q,\omega)$, which describes the response to the external probe plus the induced polarization field, consists of two terms,

$$\chi_{44}^{0,c}(q,\omega)=\alpha_4(q)\frac{n_4 q^2}{m_4^*(q)[\omega^2-\epsilon_4^2(q)+i\epsilon]}+n_4 A_4(q) \ , \tag{3.2}$$

the first term corresponding to an excitation of a (noninteracting) ^{4}He quasiparticle from the ^{4}He condensate at density n_4. The quasiparticle carries an effective mass $m_4^*(q)$ and energy $\epsilon_4(q)=q^2/2m_4^*$. The second term, $n_4 A_4(q)$, represents the static limit of the multiparticle response. The renormalization parameter $\alpha_4(q)$ and the multiparticle contribution $A_4(q)$ have been obtained from experimental data as is explained in detail in Refs. 8 and 9.

For ^{3}He one has to distinguish between coherent and incoherent contributions

$$\bar{\chi}_{33}^{c/i}(q,\omega)=\frac{\chi_{33}^{0,c/i}(q,\omega)}{1-V_{33}^{s/a}(q,\omega)\chi_{33}^{0,c/i}(q,\omega)+i\epsilon} \tag{3.3}$$

with the spin-symmetric and spin-antisymmetric polarization potentials V_{33}^s and V_{33}^a, respectively. The "screened" susceptibility $\chi_{33}^{0,c/i}(q,\omega)$ consists of a single particle contribution given by a temperature-dependent Lindhard function $L(q,\omega;m_3^*,T)$ (Ref. 14) corresponding to excitations of noninteracting quasiparticles (fermions) with an effective mass m_3^* and a multiparticle contribution $A_3^{c/i}(q)$,

$$\chi_{33}^{0,c/i}(q,\omega)=\alpha_3^{c/i}(q)n_3 L(q,\omega;m_3^*,T)+n_3 A_3^{c/i}(q) \ . \tag{3.4}$$

The temperature dependence of the present calculation stems entirely from the temperature dependence of the Lindhard function. Possible temperature dependence of the screened ^{4}He susceptibility has been neglected. Furthermore, it is emphasized that the screened susceptibilities are determined in the free-gas approximation so that $\chi^0_{34}=0$.

Interactions between the ^{3}He and ^{4}He channels are introduced via

$$\chi^c_{44}(q,\omega)=\frac{\bar{\chi}^c_{44}(q,\omega)}{1-V^2_{34}(q,\omega)\bar{\chi}^c_{33}(q,\omega)\bar{\chi}^c_{44}(q,\omega)+i\epsilon}\ , \tag{3.5a}$$

$$\chi^c_{34}(q,\omega)=\frac{\bar{\chi}^c_{33}(q,\omega)V_{34}(q,\omega)\bar{\chi}^c_{44}(q,\omega)}{1-V^2_{34}(q,\omega)\bar{\chi}^c_{33}(q,\omega)\bar{\chi}^c_{44}(q,\omega)+i\epsilon}\ , \tag{3.5b}$$

$$\chi^c_{33}(q,\omega)=\frac{\bar{\chi}^c_{33}(q,\omega)}{1-V^2_{34}(q,\omega)\bar{\chi}^c_{33}(q,\omega)\bar{\chi}^c_{44}(q,\omega)+i\epsilon} \tag{3.5c}$$

assuming $V_{34}=V_{43}$. These equations are equivalent to the matrix equations used by Pedersen and Cowley.[5]

A simple conclusion can be drawn immediately from these equations: Inserting Eq. (3.3) into Eq. (3.5c) one obtains after a little algebra

$$\chi^c_{33}=\frac{\chi^{0,c}_{33}}{1-V_0\chi^{0,c}_{33}} \tag{3.6}$$

with

$$V_0=V^s_{33}+V^2_{34}\bar{\chi}^c_{44}\ . \tag{3.7}$$

The ^{3}He quasiparticles effectively interact via the potential V_0, which is the sum of the "direct" interaction V^s_{33} and the phonon exchange interaction $V^2_{34}\bar{\chi}^c_{44}$. It has been shown by Bardeen, Baym, and Pines[1] that these two interactions nearly cancel each other in dilute mixtures. In fact, for dilute mixtures and $q,\omega\to 0$, V_0 is weakly attractive, while V^s_{33} and V_{34} are strongly repulsive.

For practical calculations we rewrite Eqs. (3.5) as follows:

$$\chi^c_{44}=\frac{\chi^{0,c}_{44}}{D}-\frac{\chi^{0,c}_{44}V_{33}\chi^{0,c}_{33}}{D}\ , \tag{3.8a}$$

$$\chi^c_{34}=\frac{\chi^{0,c}_{44}V_{34}\chi^{0,c}_{33}}{D}\ , \tag{3.8b}$$

$$\chi^c_{33}=\frac{\chi^{0,c}_{33}}{D}-\frac{\chi^{0,c}_{44}V_{44}\chi^{0,c}_{33}}{D}\ , \tag{3.8c}$$

with

$$D=1-V_{44}\chi^{0,c}_{44}-V^s_{33}\chi^{0,c}_{33}+(V^s_{33}V_{44}-V^2_{34})\chi^{0,c}_{33}\chi^{0,c}_{44}+i\epsilon\ . \tag{3.9}$$

For $V^s_{33}=V_{44}=V_{34}$ the last term in Eq. (3.9) drops out. In fact, in ^{3}He-^{4}He mixtures V_{33}, V_{34}, and V_{44} are of similar strength, and Pedersen and Cowley have set them equal in their calculations.[5] This approximation can be somewhat improved as will be explained in the following section.

For certain q and ω the imaginary part of $\chi^{0,c}_{33}$ is zero or very small. In this situation we obtain two well-separated peaks, one of which is sharp. The position of this peak is determined from Eq. (3.9) by setting $\mathrm{Re}D=0$:

$$(\bar{\chi}^c_{44})^{-1}-V^2_{34}\bar{\chi}^c_{33}=0\ . \tag{3.10}$$

Superficially this equation looks identical to the result obtained by Hsu, Pines, and Aldrich (HPA) [Eq. (3.8) in Ref. 6]. However, there is an important difference: HPA calculate $\bar{\chi}_{33}$ with the potential V_0 defined in Eq. (3.6), which is very weak for dilute mixtures. Instead, V^s_{33} should be used, and this potential is rather strong. The procedure followed by HPA does not treat phonon exchange consistently.

At this point another remark concerning the work of HPA (Ref. 6) is in order: HPA neglect χ^c_{34}. While this does not affect the determination of the peak position [see Eq. (3.9)], consideration of this term is crucially important for the determination of the peak strength.

IV. POLARIZATION POTENTIALS AND EFFECTIVE MASSES

Essential ingredients of the polarization potential approach are a number of phenomenological parameters: the effective masses m_i^*, the polarization potentials V_{ij}, and the multiparticle and renormalization parameters A_i and α_i. This is a formidable set of parameters and nothing much would have been achieved if they were completely free and independent. In fact, here we do not determine any new parameters, but want to employ those determined by Aldrich and Pines for pure ^{3}He (Ref. 8) and pure ^{4}He (Ref. 9) suitably extrapolated for the present calculation of ^{3}He-^{4}He mixtures.

The polarization potentials can be separated into a scalar and vector part corresponding to coupling to the density and current density, respectively,

$$V_{ij}(q,\omega)=f_{ij}(q)+\frac{\omega^2}{q^2}g_{ij}(q)\ . \tag{4.1}$$

For ^{3}He we also distinguish between spin-symmetric potentials f^s_{ij},g^s_{ij} and spin-antisymmetric potentials f^a_{ij},g^a_{ij}. The polarization potentials are effective quantities (pseudopotentials), which in principle depend on density, concentration, and temperature. The determination of these potentials is complicated and involves consideration of various experimental results as, e.g., Landau parameters obtained from thermodynamic data.

Unfortunately, even for $\bar{\chi}_{44}$ we cannot take over directly the potentials determined for pure ^{4}He, since the ^{4}He density n_4 changes due to the presence of the ^{3}He atoms. In order to compare our calculation with available experimental data we need a model of the variation of the different potentials with density. At present, we do not have such a model at our disposal and must rely on suitable approximations. It has been noted by Pedersen and Cowley,[5] that the polarization potentials vary approximately linearly with total density n,

$$f_{ij}(q)=\frac{f^{\mathrm{SVP}}_{44}(q)-f^{\mathrm{SVP}}_{33}(q)}{n^{\mathrm{SVP}}_4-n^{\mathrm{SVP}}_3}(n-n^{\mathrm{SVP}}_4)+f^{\mathrm{SVP}}_{44}(q)\ . \tag{4.2}$$

An analogous Ansatz is taken for $g_{ij}(q)$. The superscript SVP indicates that the quantity is determined at saturated vapor pressure of pure ^{3}He (Ref. 8) or ^{4}He,[9] respectively. Incidentally, in the measurements of Fåk *et al.*,[7] pressure has been applied such that $n \approx n_4^{\rm SVP}$ for different concentrations x_3, i.e., in this case $f_{ij}(q)=f_{44}^{\rm SVP}(q)$ according to Eq. (4.2). It is assumed implicitly in Eq. (4.2) that $f_{33}=f_{34}=f_{44}$. However, this is not consistent with the results of Bardeen, Baym, and Pines[1] for dilute mixtures. They show that for $q\to 0$, $f_{33}=(1+2\alpha)f_{44}$, $f_{34}=(1+\alpha)f_{44}$, and $f_{33}f_{44}-f_{34}^2=-\alpha^2 f_{44}^2$, where $\alpha=0.28$ is the relative increase in effective volume resulting from the replacement of a ^{4}He atom by a ^{3}He atom. We use these relations between the potentials f_{ij} for all q.

For pure ^{3}He and ^{4}He the effective mass is related to the bare mass m_i and to the vector polarization potential via $m_i^*(q)=m_i+n_i g_{ii}(q)$. The term $n_3 g_{33}(q)$ is, however, very small in dilute mixtures of ^{3} He in ^{4}He. More important is the correction to the ^{3}He mass resulting from "dressing up with a ^{4}He cloud,"

$$m_3^* = m_3 + n_3 g_{33}(q) + n_4 a_{34}(q) \tag{4.3a}$$

and analogously

$$m_4^* = m_4 + n_4 g_{44}(q) + n_3 a_{43}(q)\ . \tag{4.3b}$$

For dilute mixtures of ^{3}He in ^{4}He the last term in Eq. (4.3b) may be safely neglected. Calculation of a_{34} is difficult, and we will use here the effective mass as determined by thermodynamic measurements[15] with a concentration dependence as given in Ref. 1.

The parameters α_3 and A_3 in pure ^{3}He turn out to be quantitatively similar to α_4 and A_4 in pure ^{4}He.[8,9] For this reason we will set them equal in this calculation and do not consider any density or concentration dependence. Numerical values are taken from Refs. 8 and 9.

V. RESULTS AND COMPARISON WITH EXPERIMENTAL DATA

Fåk *et al.* recently measured dynamic structure factors of ^{3}He-^{4}He mixtures at temperatures between 0.07 and 0.9 K for ^{3}He concentrations of 1 and 5% and for momentum transfers between 9 and 17 nm^{-1} (Fig. 1). We shall call the lower energy peak of the structure factor *P*-1 and the higher energy peak *P*-2. In previous publications (e.g., Ref. 7) *P*-1 has been called particle-hole peak and *P*-2 phonon-roton peak; we do not, however, follow this convention since—as shown below—S_{33}, S_{44}, and S_{34} contribute significantly to both peaks. For the present comparison of the calculations with the data it is enough to consider three important characteristics of each peak: strength (μ_0), peak position ($\omega_0=\mu_1/\mu_0$), and peak width [$\Gamma=2\sqrt{(\mu_2/\mu_0-\mu_1^2/\mu_0^2)}$]. These characteristics are calculated from the moments $\mu_n=\int d\omega\omega^n S(q,\omega)$, where the integral extends over *P*-1 or *P*-2, respectively. Above about $q=15$ nm^{-1} the two peaks overlap and separate moments cannot be defined. This kinematic region will be discussed at the end of this section.

In Fig. 2 we compare the calculated with the measured peak positions for a 5% mixture at 0.07 K with density $n=21.97$ nm^{-3}. The calculated position of *P*-2 is found to be somewhat above the data. Therefore, the present calculation predicts a shift of *P*-2 from its position for pure ^{4}He at the same density which is too big. The calculated position of the *P*-1 is slightly below the data for q smaller than 13 nm^{-1}. The present calculation has been done with a constant (i.e., q independent) ^{3}He effective mass as described in the previous section. Agreement between data and calculation could be improved by choosing a q-dependent effective mass m_3^* as has been used, e.g., in Ref. 16.

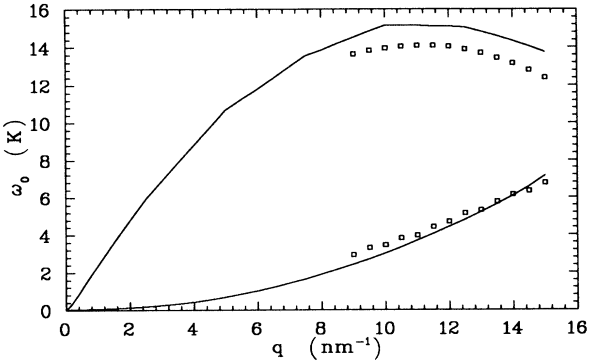

FIG. 2. Comparison of the measured peak position (squares) with the calculated peak position (full line). Upper curve: *P*-2. Lower curve: *P*-1. ($x_3=5\%$, $T=0.07$ K, $n=21.97$ nm^{-3}.)

HPA obtained significantly smaller shifts of *P*-2 in better agreement with experiment. Therefore, this problem must be addressed in more detail. As was pointed out in Sec. III one obtains the position of *P*-2 from Re$D=0$ if Im$\chi_{33}^{0,c}=0$. Therefore, for $n\approx n_4^{\rm SVP}$ (as has been assured in the experiments) a peak at the same position as for pure ^{4}He at SVP would be obtained if $V_{33}^s\chi_{33}^{0,c}-(V_{33}^s V_{44}-V_{34}^2)\chi_{33}^{0,c}\chi_{44}^{0,c}=0$. The second term in this expression ($\sim\alpha^2$ as shown in the previous section) is small compared to the first term. The peakshift is therefore essentially determined by $V_{33}^s\chi_{33}^{0,c}$. This term is rather big in the maxon region and drops to zero in the roton re-

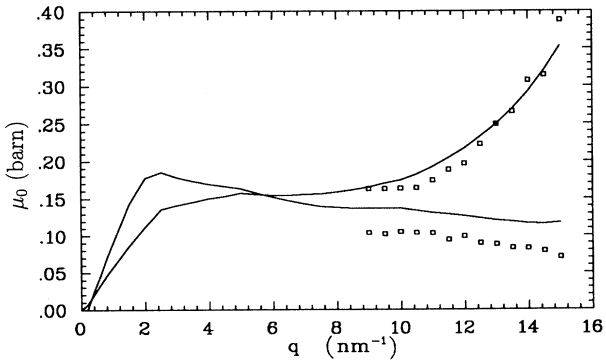

FIG. 3. Comparison of the measured peak strength (squares) with the calculated peak strength (full line). Upper curve: *P*-2. Lower curve: *P*-1. ($x_3=5\%$, $T=0.07$ K, $n=21.97$ nm^{-3}.)

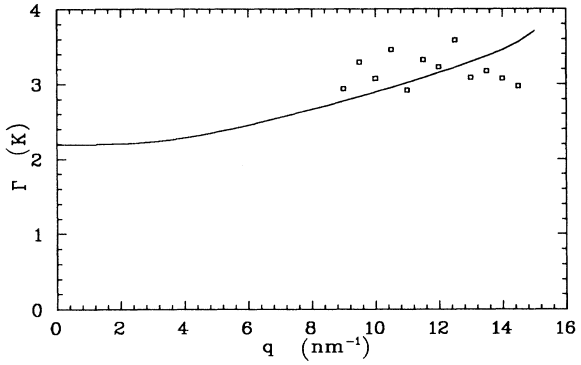

FIG. 4. Comparison of the measured (squares) with the calculated peak width of P-1. ($x_3=5\%$, $T=0.07$ K, $n=21.97$ atoms/nm^3.)

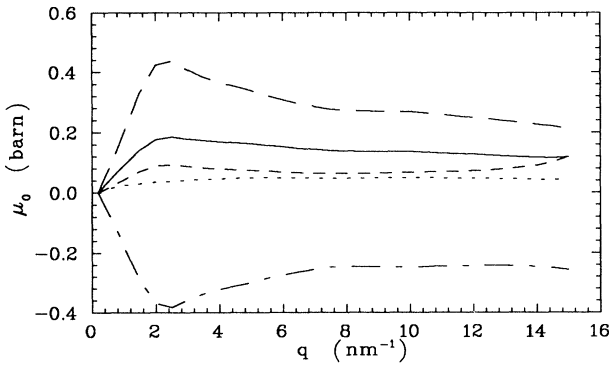

FIG. 6. Contribution of $\sigma^c_{33}S_{33}$, $2\sigma^c_{34}S^c_{34}$, $\sigma^c_{44}S^c_{44}$, and $\sigma^i_{33}S^i_{33}$ to the zeroth moment of P-1. Convention of the plotting symbols as in Fig. 5. ($x_3=5\%$, $T=0.07$ K, $n=21.97$ nm^{-3}.)

gion, since V^s_{33} vanishes there. HPA obtained smaller shifts in the maxon region since they inconsistently replaced V^s_{33} by V_0 as has been discussed in Sec. III. On the other hand, it is experimentally without doubt that the peakshift is small. It is the real part of $\chi^{0,c}_{33}$ of the HPA formulation we employ here which most probably needs revision, since contributions corresponding to virtual multiparticle excitations have only been included in the static limit. This issue will be addressed in a forthcoming publication.

In Fig. 3 we compare the calculated strength μ_0 of both peaks with the experimental data. The q dependence of μ_0 is reproduced quite satisfactorily. As observed experimentally μ_0 of P-1 decreases with increasing q. In a quasifree Fermi gas model the particle-hole strength would be constant above $2k_F$. In the present calculation strength from P-1 is shifted to P-2 peak as will be discussed in more detail below.

The measured and calculated widths of P-1 are compared in Fig. 4. An experimental resolution of 1.2 K is quadratically added to the calculated width. The data indicate that the width increases with increasing q. This q dependence is confirmed by the calculation.

In Fig. 5 we show for $q=11$ nm^{-1} the structure factor and its four contributions $\sigma^c_{33}S^c_3$, $2\sigma^c_{34}S^c_{34}$, $\sigma^c_{44}S^c_{44}$, and $\sigma^i_{33}S^i_{33}$. The very large and *negative* contribution of S^c_{34} to P-1 is surprising. Part of the strength removed by S^c_{34} from P-1 appears as a *positive* contribution to P-2. Moreover, the contributions of S^c_{44} and S^i_{33} to P-1 are quite sizable. These facts clearly indicate that P-1 of the structure factor of a ^{3}He-^{4}He mixture cannot be explained by particle-hole excitations alone. Exchange of virtual phonons plays a very important role. Conversely, virtual particle-hole excitations provide significant strength in P-2. The calculated structure factor is folded with a Gaussian to account for experimental resolution. The width of the Gaussian is 1.2 K, i.e., the width of P-2 shown in Fig. 5 is purely resolution. However, the strength of this peak is determined by the present calculation without any adjustments. Obviously, the qualitative agreement with the measured spectrum in Fig. 1 is satisfactory. We have made no attempt to "fine tune" parameters for this calculation. To force quantitative agreement with the data would not be useful at this point.

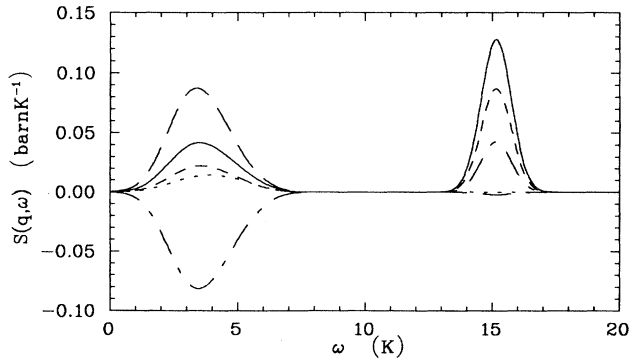

FIG. 5. Calculated structure factor for $q=11$ nm^{-1}. The full line represents $S(q,\omega)$, the long dashed line $\sigma^c_{33}S^c_{33}$, the dashed-dotted line $2\sigma^c_{34}S^c_{34}$, the short dashed line $\sigma^c_{44}S^c_{44}$, and the dotted line $\sigma^i_{33}S^i_{33}$. ($x_3=5\%$, $T=0.07$ K, $n=21.97$ nm^{-3}.)

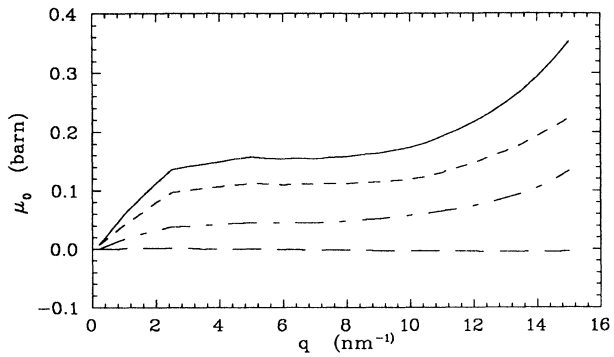

FIG. 7. Contribution of $\sigma^c_{33}S^c_{33}$, $2\sigma^c_{34}S^c_{34}$, and $\sigma^c_{44}S^c_{44}$ to the zeroth moment of P-2. Convention of the plotting symbols as in Fig. 5. ($x_3=5\%$, $T=0.07$ K, $n=21.97$ nm^{-3}.)

An overview on the separate contributions of $\sigma^c_{33}S^c_{33}$, $2\sigma^c_{34}S^c_{34}$, $\sigma^c_{44}S^c_{44}$, and $\sigma^i_{33}S^i_{33}$ to P-1 and P-2 is presented in Figs. 6 and 7. Here we have plotted the zeroth moment of each contribution separately. These figures indicate that the discussion above for $q=11$ nm^{-1} applies for all q.

In Fig. 8 results of the calculation for $q=17$ nm^{-1} are presented. Here the complicated interference of particle-hole and phonon-roton dynamics is even more obvious. The figure clearly demonstrates that it is not sensible to separate off a particle-hole peak from the data by suitably fitting the measured peak by two overlapping Gaussians as has been attempted in Ref. 16. Again, the calculated peak position is somewhat too high for quantitative agreement with the data. The data show a single peak with a less-pronounced shoulder than the calculation on the low energy side.[16]

A more refined model for the polarization potentials, effective masses, and multiparticle parameters than employed in this paper would be certainly desirable. This could improve quantitative agreement of calculation and data. Furthermore, the treatment of multiparticle excitations needs improvement: The multiphonon continuum which is apparent in the data above P-2 (see Fig. 1) has not been addressed in the present calculation. However, much more important for the energy regime considered in this paper is the consideration of virtual multiparticle excitations in the real part of $\bar{\chi}_{33}$ and $\bar{\chi}_{44}$ beyond the static limit. These contributions may be essential to achieve better quantitative agreement between data and calculation. Moreover, sum rules can only sensibly be calculated after multiparticle contributions have been included. In the present calculation the f-sum rule, for example, is badly violated in the maxon region.

In summary, an attempt has been made to describe the density-density response of ^{3}He-^{4}He mixtures at low temperatures within the polarization potential approach. The calculation achieves reasonable qualitative agreement with data recently measured by Fåk *et al.* More importantly, it is shown that both peaks of the response function are significantly influenced by particle-hole and phonon-roton excitations alike, and that the notion that the lower energy peak of the response function essentially stems from quasifree particle-hole excitations is too naive.

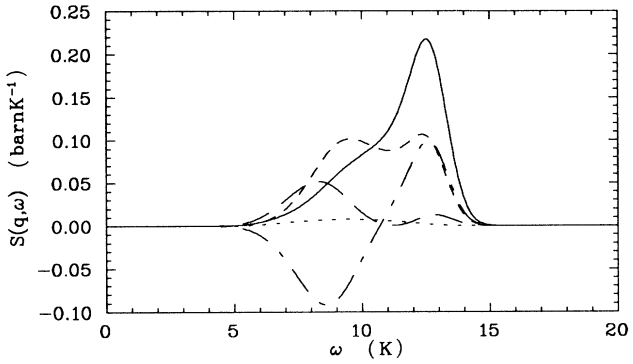

FIG. 8. Calculated structure factor for $q=17$ nm^{-1}. Convention of the plotting symbols as in Fig. 5. ($x_3=5\%$, $T=0.07$ K, $n=21.97$ nm^{-3}.)

ACKNOWLEDGMENTS

We would like to thank Ph. Nozières and R. Scherm for their hospitality at Institut Laue Langevin (ILL) in Grenoble and Ph. Nozières for a very helpful suggestion. Many useful conversations with K. Guckelsberger, who provided the experimental data in the form reported here, are gratefully acknowledged. We thank B. Fåk for a critical reading of the manuscript. M.W. would like to thank the European Science Foundation for a travel grant to visit ILL.

[1] J. Bardeen, G. Baym, and D. Pines, Phys. Rev. **156**, 207 (1967).
[2] J. M. Rowe, D. L. Price, and G. E. Ostrowski, Phys. Rev. Lett. **31**, 510 (1973).
[3] P. A. Hilton, R. Scherm, and W. G. Stirling, J. Low Temp. Phys. **27**, 851 (1977).
[4] M. Lücke and A. Szprynger, Phys. Rev. B **26**, 1374 (1982); A. Szprynger and M. Lücke, Phys. Rev. B **32**, 4442 (1985).
[5] K. S. Pedersen and R. A. Cowley, J. Phys. C **16**, 2671 (1983).
[6] W. Hsu, D. Pines, and C. H. Aldrich III, Phys. Rev. B **32**, 7179 (1985).
[7] B. Fåk, K. Guckelsberger, M. Körfer, R. Scherm, and A. J. Dianoux, Phys. Rev. B **41**, 8732 (1990).
[8] C. H. Aldrich III and D. Pines, J. Low Temp. Phys. **32**, 689 (1978).
[9] C. H. Aldrich III and D. Pines, J. Low Temp. Phys. **25**, 677 (1976).
[10] J. Boronat, F. Dalfovo, F. Mazzanti, and A. Polls, Phys. Rev. B **48**, 7409 (1993).
[11] H. R. Glyde and E. C. Svensson, in *Neutron Scattering*, Vol. 23B of *Methods in Experimental Physics*, edited by D. L. Price and K. Sköld (Academic, New York, 1987), p. 303.
[12] V. F. Sears, in *Neutron Scattering*, Vol. 23A of *Methods in Experimental Physics* (Ref. 11), p. 533.
[13] K. Guckelsberger, W. Nistler, R. Scherm, and M. Weyrauch (unpublished).
[14] J. Lindhard, K. Danske Vindensk. Selsk. Mat.-Fys. Meddr. **28**, 8 (1954); F. C. Khanna and H. R. Glyde, Can. J. Phys. **54**, 648 (1976).
[15] D. O. Edwards, D. F. Brewer, P. Seligman, M. Skertic, and M. Yaqub, Phys. Rev. Lett. **15**, 773 (1965); E. Polturak and R. Rosenbaum, J. Low Temp. Phys. **43**, 477 (1981).
[16] R. Scherm, K. Guckelsberger, A. Szprynger, and B. Fåk, J. Low Temp. Phys. **93**, 57 (1993).